Advantages of closed-loop calibration in intracortical brain–computer interfaces for people with tetraplegia

2013 J. Neural Eng. 10 046012

(http://iopscience.iop.org/1741-2552/10/4/046012)

J. Neural Eng. **10** (2013) 046012 (10pp) doi:10.1088/1741-2560/10/4/046012

Advantages of closed-loop calibration in intracortical brain–computer interfaces for people with tetraplegia

Beata Jarosiewicz[1,2,3], **Nicolas Y Masse**[1,2,8], **Daniel Bacher**[2,4], **Sydney S Cash**[5], **Emad Eskandar**[6], **Gerhard Friehs**[7,9], **John P Donoghue**[1,2,3,4] **and Leigh R Hochberg**[2,3,4,5]

[1] Department of Neuroscience, Brown University, 2 Stimson Ave., Box 1994, Providence, RI 02912, USA
[2] Brown Institute for Brain Science, Brown University, 2 Stimson Ave., Box 1953, Providence, RI 02912, USA
[3] Center for Neurorestoration and Neurotechnology, Rehabilitation R&D Service, Department of Veterans Affairs Medical Center, Providence, RI, USA
[4] School of Engineering, Brown University, 2 Stimson Ave., Box 1994, Providence, RI 02912, USA
[5] Neurology, Massachusetts General Hospital, Harvard Medical School, Boston, MA, USA
[6] Neurosurgery, Massachusetts General Hospital, Harvard Medical School, Boston, MA, USA
[7] Department of Neurosurgery, Rhode Island Hospital, Providence, RI, USA

E-mail: beata@brown.edu

Received 18 January 2013
Accepted for publication 19 June 2013
Published 10 July 2013
Online at stacks.iop.org/JNE/10/046012

Abstract

Objective. Brain–computer interfaces (BCIs) aim to provide a means for people with severe motor disabilities to control their environment directly with neural activity. In intracortical BCIs for people with tetraplegia, the decoder that maps neural activity to desired movements has typically been calibrated using 'open-loop' (OL) imagination of control while a cursor automatically moves to targets on a computer screen. However, because neural activity can vary across contexts, a decoder calibrated using OL data may not be optimal for 'closed-loop' (CL) neural control. Here, we tested whether CL calibration creates a better decoder than OL calibration even when all other factors that might influence performance are held constant, including the amount of data used for calibration and the amount of elapsed time between calibration and testing. *Approach*. Two people with tetraplegia enrolled in the BrainGate2 pilot clinical trial performed a center-out-back task using an intracortical BCI, switching between decoders that had been calibrated on OL versus CL data. *Main results*. Even when all other variables were held constant, CL calibration improved neural control as well as the accuracy and strength of the tuning model. Updating the CL decoder using additional and more recent data resulted in further improvements. *Significance*. Differences in neural activity between OL and CL contexts contribute to the superiority of CL decoders, even prior to their additional 'adaptive' advantage. In the near future, CL decoder calibration may enable robust neural control without needing to pause ongoing, practical use of BCIs, an important step toward clinical utility.

(Some figures may appear in colour only in the online journal)

[8] Present address: Department of Neurobiology, University of Chicago, Chicago, IL, USA.
[9] Present address: American Medical Center, Nicosia, Cyprus.

1. Introduction

Conventional assistive devices for people with severe motor disabilities are inherently limited, often relying on residual motor function for their use. Brain–computer interfaces (BCI) and brain–machine interfaces (BMI), sometimes collectively called neural interface systems (NIS), are being developed to provide a more powerful control signal by decoding movement intentions in real time directly from neural activity (Burrow *et al* 1997, Chapin *et al* 1999, Serruya *et al* 2002, Taylor *et al* 2002, Hochberg *et al* 2006, 2012, Santhanam *et al* 2006, Velliste *et al* 2008, Jarosiewicz *et al* 2008, Kim *et al* 2008, Ganguly and Carmena 2009, Simeral *et al* 2011, Hauschild *et al* 2012, Collinger *et al* 2013). Intracortical BCIs have permitted people with tetraplegia to control cursors on computer screens, robotic arms, and other prosthetic devices by simply imagining movements of their own arms (Hochberg *et al* 2006, 2012, Kim *et al* 2008, Simeral *et al* 2011, Collinger *et al* 2013).

Because it is not possible to map neural activity to actual arm movements in people with tetraplegia, in many previous human intracortical BCI studies the decoder has been calibrated using imagined arm movements (Hochberg *et al* 2006, Simeral *et al* 2011). Specifically, the participant was asked to imagine moving a mouse with his or her hand to guide a cursor that automatically moved to targets displayed on a computer screen while neuronal ensemble activity was recorded from a 96-microelectrode array implanted in the participant's motor cortex. A decoder was then created by mapping the recorded patterns of neural activity to the computer-generated cursor movements. This decoder calibration procedure is termed 'open-loop' (OL) because the participant does not receive any feedback about his or her neural activity. Subsequently, this 'OL decoder' is used to infer movement intention from neural activity in real time, allowing the participant to control the motion of the cursor by simply imagining moving his or her arm. This is termed 'closed-loop' (CL) neural control because the participant receives real-time visual feedback of the effect of his or her neural activity on cursor motion.

A potential shortcoming of using an OL decoder for CL neural control is that the relation between neural activity and movement intention can vary with changes in context. For example, the directional tuning of motor cortical neurons in able-bodied monkeys can differ when cursor movement is hand controlled compared to when it is neurally controlled (Taylor *et al* 2002, Carmena *et al* 2003, Lebedev *et al* 2005, Ganguly *et al* 2011). Similar context-dependent changes in neural tuning have also been reported in motor cortex of people with tetraplegia switching from a two-cursor hybrid OL/CL decoder calibration task to purely CL neural control (Kim *et al* 2008). If neural activity differs between OL decoder calibration and CL neural control, then an OL decoder will not be optimal for CL neural control. Additionally, the participant may not be as mentally engaged during OL imagination of movement as she/he would be during CL neural control, potentially further reducing the quality of a decoder calibrated on OL data.

Furthermore, the relationship between movement intention and neural activity can change over time because of physiological and/or recording nonstationarities in the neural signals (Kim *et al* 2006, Wessberg and Nicolelis 2006, Santhanam *et al* 2007, Chestek *et al* 2011, Perge *et al* 2013). If only OL calibration were available, BCI use would have to be interrupted to recalibrate the decoder when such nonstationarities occur. Adaptive decoding has been proposed and used successfully as a solution to the signal nonstationarity problem by using data acquired during ongoing CL neural control to periodically or continuously recalibrate the decoder (for reviews, see Millán *et al* 2007, Berger *et al* 2010, Schlögl *et al* 2010).

In continuous spike-based BCIs such as the one used in this study, various adaptive decoding methods have been tested in CL neural control in able-bodied non-human primates (Taylor *et al* 2002, Helms Tillery *et al* 2003, Wahnoun *et al* 2006, Jarosiewicz *et al* 2008, Velliste *et al* 2008, Shpigelman *et al* 2009, Li *et al* 2011, Gilja *et al* 2012, Orsborn *et al* 2012, Sussillo *et al* 2012) and in people with tetraplegia (Hochberg *et al* 2012, Collinger *et al* 2013). In these studies, the decoder was initialized in OL by mapping neural activity to hand movements, to observed target presentations, or to observed effector movements. The decoder was then recalibrated using data acquired during CL neural control. In a subset of these intracortical studies (Helms Tillery *et al* 2003, Shpigelman *et al* 2009, Li *et al* 2011, Gilja *et al* 2012, Sussillo *et al* 2012), the quality of neural control using the 'CL decoder' was compared to the quality of neural control using the original OL decoder, and in each case, the CL decoder outperformed the OL decoder. However, none of these studies were designed to distinguish among the multiple possible contributions to the superiority of CL decoders, which could include (1) differences in neural activity during the OL versus CL calibration tasks, (2) increased mental engagement during CL, (3) the inclusion of more calibration data in the CL decoder, and/or (4) the ability of CL decoders to adapt to signal nonstationarities.

To disambiguate among these contributions to the superiority of CL decoders, we compared the quality of neural control and the strength and accuracy of the neural tuning models obtained using OL versus *balanced* CL decoder calibration in people with tetraplegia performing a two-dimensional (2D) center-out task using an intracortical spike-based BCI (figure 1(A)). We found that CL decoders improved neural control relative to OL decoders even when the two decoders were balanced for the total amount of data used in their calibration, thereby excluding a possible contribution from item 3 above (the ability to include more data in CL decoder calibration). They were also balanced for the amount of elapsed time between calibration and testing, thereby excluding a possible contribution from item 4 above (the ability of CL decoders to adapt to signal nonstationarities). Directional tuning differed between OL and CL contexts, suggesting that eliminating context differences between decoder calibration and neural control (item 1 above) contributed to the performance improvement when using a CL decoder. Directional tuning was also significantly

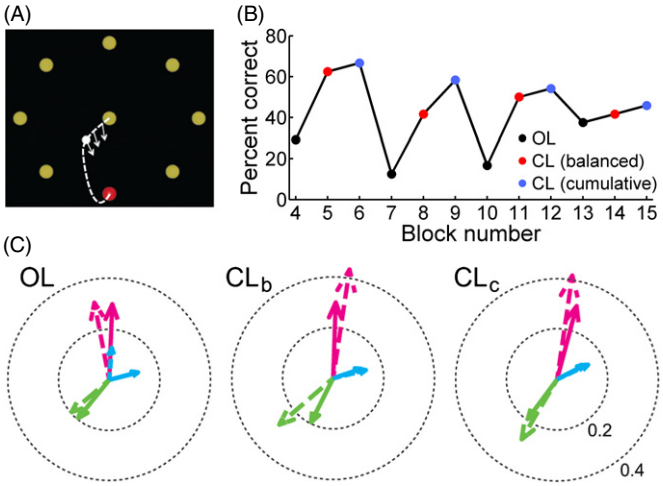

Figure 1. Methods and example data. (A) The center-out-back task. Possible target locations are shown as yellow dots that turn red when they become active. After reaching a peripheral target, the participant must bring the cursor back to the center target before the next peripheral target becomes active. To obtain a tuning model from data acquired during CL control, at each moment along the cursor's trajectory (*white dotted line*) toward each active target, the person's intended movement direction is assumed to be from the current cursor location (*white dot*) toward the active target location (*red dot*). The normalized direction vectors (*white arrows)* were regressed against neural activity in each 100 ms bin from the initial, 'ballistic' portion of each trial to obtain a model of each unit's directional tuning. This method was used both for in-session CL decoder calibration and for post-hoc analysis. (B) Example performance data from participant S3, 1966 days post-implant, showing the percentage of targets successfully acquired in each 3–5 min CL 'block' of 24 target presentations. Each dot is color-coded according to whether the decoder used in that block was an OL decoder (*black*), a CL_b decoder (*red*), or a CL_c decoder (*blue*). Decoder types were interleaved throughout each session to control for elapsed time since decoder calibration and other time-varying factors. (C) Examples of preferred directions (PDs) from the same session. Each color (*magenta, blue, green*) represents one unit. The dashed arrow of that color represents the PD used by the decoder for that unit (H_i) and the solid arrow of the same color represents the PD obtained post-hoc for that unit from the blocks in which that decoder was used. The left plot shows three units in the OL decoder blocks, the middle plot shows the same three units in the CL_b decoder blocks, and the right plot shows the same three units in the CL_c decoder blocks. The length of each solid arrow represents the unit's whole-session PD NMI (see section 2.5). Similarly, the length of each dotted arrow represents that unit's decoder NMI. As exemplified most clearly by the blue unit, the narrowing of the angle between the model and post-hoc PD in the CL blocks is a measure of improved model accuracy.

stronger during CL than during OL, suggesting an additional contribution from increased mental engagement during CL than during OL (item 2 above). Because the decoders were interleaved across blocks within each recording session, these improvements are unlikely to be attributable to uncontrolled time-varying factors. Harnessing the full adaptive potential of CL decoders by recalibrating them with additional and more recent data (i.e. including possible contributions from items 3 and 4), as could be done in practical BCI use, resulted in further improvements in tuning model accuracy and in neural control.

2. Methods

2.1. Participants

Permission for these studies was granted by the US Food and Drug Administration (Investigational Device Exemption[10]) and the Partners Healthcare/Massachusetts General Hospital Institutional Review Board. The two participants in this study (S3 and T1) were enrolled in a pilot clinical trial of the BrainGate2 Neural Interface System (www.clinicaltrials.gov/ct2/show/NCT00912041), and were implanted with a 96-channel intracortical silicon microelectrode array (Cyberkinetics Neurotechnology Systems, Inc., now Blackrock Microsystems, Salt Lake City, UT), as previously described (Hochberg *et al* 2006, Simeral *et al* 2011).

Participant S3 is a 58-year-old woman with tetraplegia and anarthria (inability to speak) resulting from a pontine stroke that occurred 9 years prior to array implantation. She retains eye movement, some head movement and facial expression, and breathes spontaneously. She has bilateral upper extremity flexor spasms that occur sporadically with many intended body movements. The array, which had electrodes 1.5 mm in length, was implanted in the hand area of her dominant motor cortex ~5 years prior to the start of this research project (see Simeral *et al* 2011, Hochberg *et al* 2012 for additional detail). Participant T1 was a 48-year-old woman with tetraplegia resulting from amyotrophic lateral sclerosis, diagnosed 6 years prior to array implantation. She was completely paralyzed except for some eye movement, and her breathing was assisted by a ventilator. The array, with electrodes 1.0 mm in length, was implanted in her dominant motor cortex ~9 months prior to the start of this research project.

2.2. Signal acquisition

Neural activity was detected by the 96-channel microelectrode array and monitored via a cable that was connected to a percutaneous connector during each 2–3 h recording session. Signals were analogue filtered (fourth order Butterworth band pass with corners at 0.3 Hz and 7.5 kHz) and digitized by a 96-channel NeuroPort Neural Signal Processor (Blackrock Microsystems, Salt Lake City, UT) at 30 kilosamples per second (kS s^{-1}).

In participant T1, signals were then causally filtered with a digital fourth order 250 Hz high-pass Butterworth filter and, for each of the 96 channels, spike waveforms were manually sorted using Cerebus Central (Blackrock Microsystems, Salt Lake City, UT) into putative single neurons ('units') using window discriminators in 1.6 ms epochs that crossed a manually set amplitude threshold. Spike counts for each unit in each 100 ms bin were sent to custom-written software in Simulink (Mathworks, Natick, MA), where they were saved to disk and, in 'CL' blocks, decoded into intended movement direction for real-time neural control.

In participant S3, the 30 kS s^{-1} signals were fed in 100 ms segments through custom software written in Simulink™, where they were buffered for 4 ms to avoid edge effects

[10] CAUTION: Investigational device. Limited by federal law to investigational use.

and then non-causally band-pass filtered using a fourth order Butterworth filter with corners at 250 and 5000 Hz. The extracted signals were compared to an amplitude threshold set to −4.5 times the standard deviation of the filtered signals on each channel (for details on the non-causal filtering and threshold crossing methods, see Hochberg *et al* (2012)). The number of threshold crossing events in each 100 ms segment was saved to disk and, in CL blocks, decoded into intended movement direction for real-time neural control (see below for details).

2.3. Task design

To determine the relationship between intended movement and brain activity, we first asked the participant to watch a cursor move to targets on a computer screen in a pre-programmed 2D four-target center-out-back task and imagine that she was controlling the cursor with her own hand while her motor cortical neural activity was recorded (OL, decoder calibration). Participant S3 was asked to imagine bending her wrist in the desired cursor movement direction, as imagined wrist movement had previously been found to elicit robust responses in her recorded units. Participant T1 was asked to imagine that she was moving a mouse on a tabletop plane to control the movement of the cursor. Targets appeared one at a time on a 19″ LCD monitor (30.5 cm high and 38 cm wide) which was placed ∼56 cm in front of the participant; targets appeared at the center, at 13 cm above or below the center, or at 15 cm left or right of the center. The targets were 1.2 cm in radius (1.2° visual angle) and the cursor was 0.6 cm in radius (0.6° visual angle). Each of the four targets appeared in a random order before the set of targets was repeated. After the OL data were collected, we used these data to construct a Kalman filter (Wu *et al* 2006, Kim *et al* 2008) that mapped the observed patterns of neural activity to instantaneous target direction, which was assumed to be the person's intended movement direction (for details, see 2.4*., Kalman filter calibration*). For participant S3, the OL decoder was calibrated on data from 24 trials, each trial consisting of a 3 s excursion of the cursor from a center to a peripheral target or a peripheral to a center target followed by a 1 s target hold period. For T1, the OL decoder was calibrated on data from three OL blocks of 16 trials, with each trial consisting of a 5 s excursion with a 1 s target hold period.

In subsequent blocks, the participant was asked to perform the four-target center-out-back task under CL neural control: the participant's intended movement direction was decoded from her neural activity, and this movement intention was used to directly control the continuous movement of the cursor in real time. For a trial to be considered successful, S3 had 8 s to move the cursor to the target and hold it there for at least 500 ms. The target acquisition rate expected by chance in this task was near 0% because the cursor and targets were small relative to the size of the screen, continuous trajectories were decoded, and the cursor had to be held over the target for it to count as a successful acquisition. For participant T1, we simplified the task by increasing the trial time to 20 s and decreasing hold time to 300 ms. Also, we algorithmically discarded the component of the commanded velocity vector orthogonal to the instantaneous target direction, similar to 'deviation gain' used by Velliste *et al* (2008), which constrained the possible cursor movements at each moment in time to a single line toward and away from the current target. This effectively reduced the difficulty level of the task to that of a one-dimensional task, while still allowing a 2D model to be generated and used for neural control. Thus, for T1, the target acquisition rate expected by chance had a theoretical range of 0% to 50%, depending on the amount and direction of bias in cursor motion. Because the baseline performance levels were expected to vary across participants and across days due to any number of uncontrolled factors, all statistical analyses were done on *relative* performance measures that were normalized to baseline performance on each day.

For S3, the OL decoder was used in the first CL block. After the CL block finished, a 'balanced' CL (CL_b) decoder was calibrated using the neural data from the first 3 s of each trial of that CL block (see figure 1(A)), using the same total amount of data to calibrate the decoder as was used to calibrate the OL decoder. For T1, the OL decoder was used in the first three CL blocks, and the first 5 s of each trial of these three CL blocks were used to calibrate the CL_b decoder. To test whether using CL data to train the decoder improved task performance and/or the accuracy of the decoder's neural tuning model (even when the CL decoder was built from the same amount of data as the OL decoder), the CL_b decoder was used in the next block of neural control. To test whether more improvement would be obtained using a CL decoder that is calibrated on additional, more recent data, as could be done in practical use of the BCI, a third, 'cumulative' CL (CL_c) decoder was built using *all* of the CL blocks acquired up to that point; this decoder was then used for decoding in the following block.

To ensure that any changes in performance and/or model accuracy that were attributed to decoder type were not influenced by any other uncontrolled time-varying factors (amount of practice, learning, fatigue, etc), several more blocks of neural control were run, interleaving the OL, CL_b, and CL_c decoders across blocks (see figure 1(B) for an example). Each time a CL_c decoder was to be used, it was first calibrated using data from *all* of the CL blocks that had been acquired up to that point. To control for the amount of time that elapsed since decoder calibration when comparing the OL to the CL_b decoder (whose sole difference was meant to be the context under which the calibration data were collected), the OL and CL_b decoders were never recalibrated. In S3, twelve total CL blocks were run in each session, with 24 trials per block, cycling four times through the OL, the CL_b, and the CL_c decoders, in that order. In T1, 10–13 total CL blocks were run in each session, with 16 trials per block, repeating each decoder type 2–5 times in random order after the initial OL, CL_b, and CL_c blocks.

2.4. Kalman filter calibration

Movement intention was decoded from spiking activity using a steady-state Kalman filter. We briefly review its properties here; full accounts can be found in other studies (Wu *et al* 2006, Kim *et al* 2008, Malik *et al* 2011). The Kalman filter is a

recursive Bayesian estimation algorithm that infers the desired cursor state from the history of spike rates. Its 'observation model' assumes that the baseline-subtracted spike rates z are linearly related to the intended movement direction d at each time point t

$$z(t) = Hd(t) + q(t), \tag{1}$$

where H is the matrix relating spiking activity to movement direction and the error term, q, is drawn from a normal distribution with zero mean and covariance matrix Q. Its 'state model' assumes that the intended movement direction at any time evolves from the movement direction in the previous time point

$$d(t) = Ad(t-1) + w(t), \tag{2}$$

where A is the matrix relating movement directions at consecutive time points and the error term, w, is drawn from a normal distribution with zero mean and covariance matrix W.

Given equations (1) and (2), the log probability of jointly observing the set of intended motion directions, $D = \{d(1), d(2), \ldots, d(N)\}$, and the set of spike rates, $Z = \{z(1), z(2), \ldots, z(N)\}$, can be expressed as:

$$\begin{aligned}\log(P(D,Z)) &= \log(p(d(1))) + \sum_{t=2}^{N} \log(p(d(t)|d(t-1))) \\ &+ \sum_{t=1}^{N} \log(p(z(t)|d(t))) \\ &= \log(c) - \frac{N-1}{2}\log|W| - \frac{N}{2}\log|Q| \\ &- \frac{1}{2}\sum_{t=2}^{N}(d(t) - Ad(t-1))W^{-1}(d(t) - Ad(t-1))^T \\ &- \frac{1}{2}\sum_{t=1}^{N}(z(t) - Hd(t))Q^{-1}(z(t) - Hd(t))^T \end{aligned} \tag{3}$$

where c is a normalization constant. Usually, the Kalman filter is calibrated by finding the parameters H, Q, A, W that maximize this joint distribution. However, we found that fixing $A = 0.965I$ and $W = 0.03I$, where I is the identity matrix, provided a good trade-off between smoothness and responsiveness of cursor movement (Hochberg *et al* 2012). Thus, for decoder calibration, we only calculated the parameters H and Q that maximized the distribution. These two parameters have the following closed-form solutions:

$$H = \left(\sum_{t=1}^{N} z(t)\, d(t)^T\right)\left(\sum_{t=1}^{N} d(t)\, d(t)^T\right)^{-1} \tag{4}$$

$$Q = \frac{1}{N}\left(\sum_{t=1}^{N} z(t) - Hd(t)\right)\left(\sum_{t=1}^{N} z(t) - Hd(t)\right)^T. \tag{5}$$

We note that each row of H contains a 2D vector representing the Kalman filter's model of a recorded unit's preferred direction (PD); its direction corresponds to the cursor direction in which the unit's spike rate is highest (i.e. the peak of its cosine fit), and its magnitude is the unit's modulation depth (i.e. the difference in firing rate between the peak of its cosine fit and its baseline). The modeled PD vector of neuron i will be denoted as H_i.

Decoder calibration was performed in batches between blocks using data from each 100 ms bin in the first 3 s (for S3) or 5 s (for T1) of each trial after target presentation (hereafter called the decoder 'calibration data'). In OL decoder calibration, this was equivalent to the cursor movement period of each trial. In CL decoder calibration, this was meant to balance the amount of time from each trial that data were used for calibrating the CL decoders with that of the OL decoders, and also to isolate the initial, 'ballistic' portion of each trial, during which the participant's intended movement direction was less likely to be influenced by error correction. For CL calibration, data from any part of the trial in which the edge of the cursor was within 1 cm (1° visual angle) of the edge of the target were also excluded from the decoder calibration because, as the cursor gets closer to the target, small cursor movements lead to larger angular changes in target direction, making intended movement direction more difficult to infer. The neural calibration data were shifted by a small temporal delay (200 ms for S3, 300 ms for T1) relative to the kinematic calibration data to account for a reaction time between cursor position updates and neural responses; these delays were chosen because they produced the largest directional modulation in off-line analyses of previous sessions from each participant (data not shown).

2.5. Data analysis

Performance and tuning model accuracy of the OL, CL_b and CL_c decoders were compared as follows. For each session, data from all blocks in which a given decoder type was used were combined to obtain a single target acquisition rate (% correct) and model accuracy for that decoder type. For example, in the session shown in figure 1(B), blocks 4, 7, 10, and 13 were combined into one OL data point in figure 2; blocks 5, 8, 11, and 14 were combined into one CL_b data point, and blocks 6, 9, 12, and 15 were combined into one CL_c data point.

As stated above, the decoder is calibrated by estimating the PD of each unit. Intuitively, the participant's quality of neural control over the cursor will be influenced by the accuracy of these estimates. To assess model accuracy, we computed a 'model error' defined as the angular difference between the PD measured when calibrating the decoder (H_i for unit i) to the PD measured during those blocks in which that decoder was used (the 'post-hoc PD'). A smaller angle between the PDs measured when calibrating and using the decoder reflects a more accurate tuning model (figure 1(C)).

Because baseline performance and model error varied across sessions and between the two participants, statistics were performed within-session on *differences* in performance and model error metrics relative to the OL decoder blocks (see figures 2(B) and (D)). P-values were obtained for these within-session comparisons using the non-parametric Wilcoxon signed rank test. Because there is more certainty in the angular error for units with stronger directional tuning, the model error of each unit was weighted (Taylor 1996, Jarosiewicz *et al* 2008, 2012b) by its whole-session 'normalized modulation index'

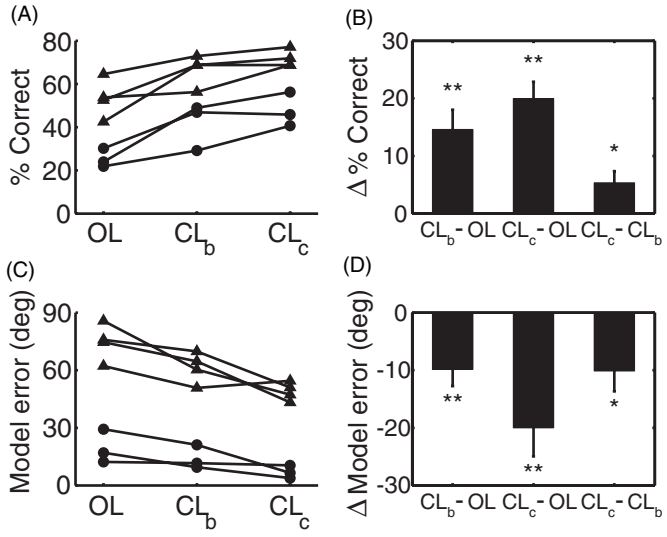

Figure 2. Improvement in performance and tuning model error with CL decoder calibration. (A) Performance data from each session from both participants. The percentage of targets acquired (% correct) across all blocks using the OL decoder, all blocks using the CL_b decoder, and all blocks using the cumulative CL_c decoder are shown for each session. Filled circles represent sessions from participant S3, and filled triangles represent sessions from participant T1 (whose version of the task was simplified; see section 2). (B) Changes in performance relative to OL, averaged across all sessions. There was a significant improvement in performance when using the CL_b and CL_c decoders compared to the OL decoders in the same session (Wilcoxon signed rank test, $p = 0.0078$). In addition, there was a significant improvement when using the CL_c decoder over using the CL_b decoder ($p = 0.031$). (C) Model error from each session from both participants. (D) Changes in model error relative to OL, averaged across all sessions. There was a significant decrease in model error (i.e. improvement in model accuracy) using the CL_b and CL_c decoders compared to the OL decoders (Wilcoxon signed rank test, $p = 0.0078$ for both CL_b and CL_c). There was also a significant improvement when using the CL_c decoder compared to the CL_b decoder ($p = 0.023$).
Key: $^* = p < 0.05$; $^{**} = p < 0.01$.

(NMI). The NMI of unit i was defined as the norm of its PD divided by the standard deviation of the residuals in the fit:

$$\frac{\|H_i\|}{\sqrt{Q_{ii}}}. \tag{6}$$

Thus, a unit with no directional tuning would have a NMI of 0, a unit whose modulation depth is equal to the standard deviation of its residuals would have a NMI of 1, and a unit whose directional modulation is larger than the standard deviation of its residuals would have a NMI greater than 1. To estimate each unit's whole-session NMI, firing rates were baseline-subtracted within each block, and then *all* of the baseline-subtracted CL calibration data from the whole session were used to obtain a single PD and NMI for that unit; this NMI was used as the weight for that unit.

Model error was also compared across decoder types treating all units from all sessions as independent samples: each unit's model error for one decoder type versus another decoder type contributed one pair of data points in a paired weighted *t*-test (Goldberg *et al* 2005, Jarosiewicz *et al* 2008, 2012b), again weighting each unit's contribution by its NMI.

To test whether CL neural control yields stronger directional modulation than OL imagined movements, we also compared the NMIs of the OL and CL decoder models themselves ('decoder NMIs'; see figure 1(C)) as a measure of how strongly modulated the units were during the blocks on which the decoders were built. The decoder NMIs were computed the same way as the post-hoc PD NMIs (using equation (6)), but they were computed for each decoder rather than for the post-hoc PD. Because NMI is sensitive to the amount of data used in its calculation, we only applied this comparison to the OL versus the CL_b decoders, which were created from matching quantities of calibration data; the CL_c decoders, which were created from more calibration data than the other decoder types, were excluded from the decoder NMI comparison.

3. Results

Across seven sessions from the two participants, the decoders calibrated on CL data provided a better target acquisition rate and a superior model fit than the decoders calibrated on OL data (figure 2). In the blocks in which the CL_b decoder was used, the target acquisition rate was 14.6 ± 3.4% higher and the model error was 9.9 ± 2.9° lower than in the blocks in which the OL decoder was used (difference in target acquisition rate, $p < 0.01$; difference in model error, $p < 0.01$, one-tailed Wilcoxon signed rank test). Recalibrating the tuning model using additional and more recent CL data resulted in further improvement of both neural control and tuning model accuracy (difference in target acquisition rate, CL_c relative to OL: 20.0 ± 2.9%; $p < 0.01$; difference in target acquisition rate, CL_c relative to CL_b = 5.4 ± 2.0%; $p < 0.05$; improvement in model error, CL_c relative to OL: 20.0 ± 4.9°; $p < 0.01$; improvement in model error, CL_c relative to CL_b: 10.1 ± 3.5°; $p < 0.05$).

Each of the above analyses treated each decoder type from each session as one data point in a pairwise analysis. To gain statistical power in comparing model accuracy across decoder types, we also computed the model error of each decoder type combining across all 251 units from all sessions (217 units from T1 and 34 units from S3), and used the difference in model error across decoder types for each cell as independent samples in a paired analysis. Across all units, the weighted mean model error was 49.9 ± 3.2° (SEM) for the OL decoders, 39.8 ± 2.6° for the CL_b decoders, and 31.8 ± 2.4° for the CL_c decoders (figure 3(A)). The CL_b decoders had significantly smaller model error than the OL decoders (mean pairwise difference, CL_b − OL: 10.2 ± 3.3°, paired *t*-test, $t = 3.12$, $p < 0.001$). Because this improvement in model error could not be attributed to differences in the amount of calibration data or the amount of elapsed time between calibration and testing, the fact that the post-hoc PDs obtained from CL blocks were more similar to the CL_b model than they were to the OL model implies that directional tuning differs between OL and CL contexts. Furthermore, the CL_c decoders had significantly smaller model error than both the OL decoders (CL_c − OL: 18.1 ± 3.6°, $t = 5.02$, $p < 10^{-7}$) and the CL_b decoders (CL_c − CL_b: 8.0 ± 2.8°;

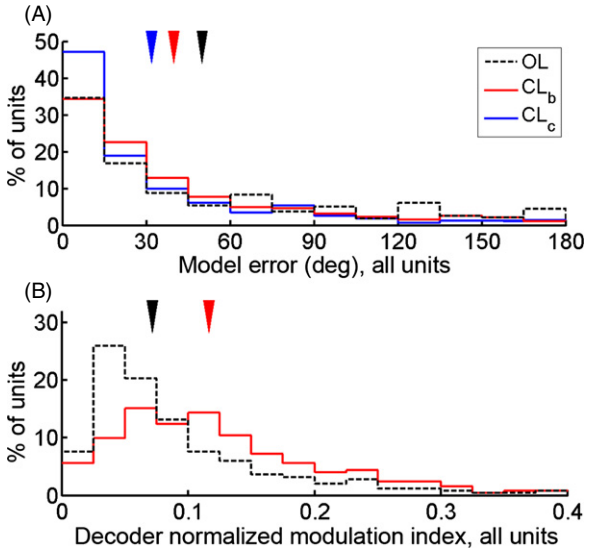

Figure 3. Model error and decoder NMI, all units from all sessions. (A) Distribution of model error, combining all units from all sessions. *Arrows* denote the weighted mean model error for each decoder type across all units. Both the CL_b decoders ($p < 0.001$) and the CL_c decoders ($p < 10^{-7}$) had significantly smaller model error than the OL decoders. Furthermore, the CL_c decoders had significantly smaller model error than the CL_b decoders ($p < 0.005$). (B) Distribution of decoder NMIs of the OL and CL_b decoders (because NMI is sensitive to the amount of data used in its calculation, the CL_c decoders were excluded from this comparison). *Arrows* denote the median for each group. The balanced CL decoder models had significantly higher modulation indices than the OL decoder models ($p < 10^{-6}$), indicating that directional tuning was stronger during CL neural control than during OL imagination of control.

$t = 2.85$; $p < 0.005$), implying that even better model accuracy can be obtained by including additional and more recent data in decoder calibration. Each of these differences were also significant for each individual participant (participant S3: $CL_b - OL$: $6.15 \pm 3.6°$, $p < 0.05$; $CL_c - OL$: $13.9 \pm 3.7°$, $p < 10^{-4}$; $CL_c - CL_b$: $7.79 \pm 2.0°$, $p < 10^{-4}$. Participant T1: $CL_b - OL$: $13.0 \pm 4.4°$, $p < 0.005$; $CL_c - OL$: $21.2 \pm 4.9°$, $p < 10^{-5}$; $CL_c - CL_b$: $8.12 \pm 3.9°$, $p < 0.05$).

The CL_b decoders also had significantly higher decoder NMIs (median = 0.12) than the OL decoders (median = 0.07; mean pairwise difference = 0.029 ± 0.006; $t = 4.67$, $p < 10^{-6}$), implying stronger directional modulation during the CL calibration task than during the OL calibration task (figure 3(B)). This difference was also significant for each individual participant (participant S3: mean pairwise difference = 0.031 ± 0.015, $t = 2.08$, $p < 0.05$; participant T1: mean pairwise difference = 0.029 ± 0.007, $t = 4.22$, $p < 10^{-5}$).

4. Discussion

When calibrating a decoder for a spike-based neural interface for people with paralysis, data acquired during CL neural control ('CL calibration') yielded a superior decoding model and better subsequent neural control than data acquired during OL imagined movements without feedback ('OL calibration'). Model error was smaller, the directional modulation was stronger, and neural control was better with CL decoders than OL decoders, even when the same amount of data were used to calibrate both decoders and when the same amount of time elapsed between each decoder's calibration and its use. Because the decoders were interleaved across blocks within each session, the observed differences are unlikely to be attributable to time-varying factors such as practice, learning, fatigue, or elapsed time since decoder calibration.

Given that neural tuning can change across different contexts (Taylor *et al* 2002, Carmena *et al* 2003, Lebedev *et al* 2005, Kim *et al* 2008, Ganguly *et al* 2011), a likely reason for the observed improvement in neural control and smaller model error using the balanced CL decoders is that CL calibration minimizes the contextual differences between decoder calibration and neural control. In BCI studies with able-bodied monkeys, if the monkeys' arms are restrained or allowed to move differently during neural control than during OL calibration, it is perhaps not surprising that MI directional tuning differs between hand control and neural control (Taylor *et al* 2002, Carmena *et al* 2003, Lebedev *et al* 2005, Ganguly *et al* 2011) given the sensitivity of motor cortical tuning to arm kinematics, dynamics, and proprioceptive feedback (Georgopoulos *et al* 1982, Schwartz *et al* 1988, Fu *et al* 1995, Sergio and Kalaska 1998, Kakei *et al* 1999, Churchland and Shenoy 2007). However, in people with tetraplegia, arm movements are absent in both OL and CL contexts, so differences in arm movements cannot explain these results. Instead, these results suggest that the activity of neurons in human MI is sensitive to the subtle distinction between imagination of movement *without* an effect on the external world (arguably a relatively 'natural' scenario) and imagination of movement *with* an effect on the external world (a scenario that has only become possible recently with the advent of BCIs).

Furthermore, the stronger directional modulation that was observed during CL neural control than during OL imagination of movement is consistent with a higher level of mental engagement during CL neural control, as increased attention, motivation, and alertness are known to increase the amount of neural activation and information present in neural activity (Edeline 2003, Reynolds and Chelazzi 2004, Roesch and Olson 2004, Chapman and Meftah 2005, Zhang *et al* 2011).

Another possible source of the observed differences in neural activity between OL and CL contexts might be additional feedback-enabled neural modulation in CL that corresponds to the user's attempts to seek strategies that improve neural control (see, e.g., Fetz 1969, 2007, Moritz *et al* 2008, Chase *et al* 2009, Koyama *et al* 2010), which does not occur during OL because such feedback is not provided. The improvements in neural control using a CL decoder, then, might be partly attributable to the incorporation of these modified neural patterns into the CL decoding model, combined with the person's continued use of similar strategies during subsequent CL neural control.

Regardless of the source of the observed improvements with CL decoders, if these improvements translate to practical BCI applications, then their functional implications are

substantial. Even before taking advantage of the 'adaptiveness' of CL decoder calibration (i.e., when using the balanced CL decoder), we observed a ∼30% relative improvement in target acquisition rate over baseline performance using the OL decoder. Using the cumulative CL decoder, we observed a ∼40% relative improvement over baseline. In a practical BCI setting, even more improvement could potentially be obtained by including more calibration data as it is collected and/or by selecting the calibration data with attention to other relevant factors such as signal nonstationarities. When neural signals are not stably recorded, the decoder could be continually recalibrated using only the most recent and relevant CL data. When the neural signals are stable over long periods of time, adding more calibration data as it is collected would continually improve the accuracy of the tuning model, and would enable more complex tuning models to be utilized that require more parameters to be fitted.

Future intracortical BCIs should provide users with control over multiple types of assistive devices over the course of a day—e.g., a computer keyboard from morning to noon, and an assistive robotic limb at mealtime. It will thus be important to understand the degree to which a decoder calibrated in one CL context (e.g., the center-out-back task) will extend to other CL contexts (e.g., a communication interface, physical devices, etc). If neural tuning also differs across different CL contexts, a decoder created during the use of one BCI application might not be optimal for another BCI application. However, preliminary work shows that the tuning model of a CL decoder calibrated in a center-out task matches the PDs obtained in a communication interface as closely as it matches the PDs obtained from other blocks of the same center-out task (Jarosiewicz *et al* 2011), suggesting that neural activity does not differ as strongly across CL contexts as between OL and CL contexts.

A crucial component of decoder calibration is knowledge of the person's movement intention, so that its relationship with the corresponding neural data can be modeled. How will this be accomplished in practical BCI applications in which targets are not pre-specified? In most conceivable practical applications of point-and-click BCIs (such as in a neural communication interface; see Bacher *et al* 2011), selections will be made by dwelling or neurally 'clicking' on possible targets on the computer screen (Kim *et al* 2011, Simeral *et al* 2011). This allows for a possible solution to the absence of *a priori* knowledge of target location: if a given selection is not followed by a corrective action (e.g., 'backspace' or 'undo'), one could infer *retrospectively* that the BCI user correctly selected his or her desired target. Once that target location is known, the person's intended movement direction during each moment of the preceding trajectory can be assumed to have been toward that target, and as before, the tuning model can be calibrated using this inference of instantaneous intended direction (Jarosiewicz *et al* 2012a). With additional constraints on the assumptions of the intended movements and on the data that would be included in decoder calibration, similar approaches for retrospective target inference guiding ongoing CL calibration could conceivably be extended to multi-dimensional neural control, such as reach and grasp control of a robotic arm (Hochberg *et al* 2012, Collinger *et al* 2013) or functional electrical stimulation of the person's own limbs (Moritz *et al* 2008, Chadwick *et al* 2011, Ethier *et al* 2012).

5. Conclusions

In two people with tetraplegia enrolled in the BrainGate pilot clinical trial, neural control was superior, and the decoder had a more accurate tuning model with a higher signal-to-noise ratio, using closed-loop (CL) decoder calibration compared to open-loop (OL) decoder calibration. CL calibration was superior even when the amount of data used to calibrate the CL decoder was balanced with the OL decoder and when the same amount of time had elapsed between each decoder's calibration and its use. These improvements are likely attributable to differences in neural activity between OL and CL contexts and to increased levels of mental engagement during CL neural control. Recalibrating the decoder using additional and more recent CL data, as could be done during practical use of the neural interface system, resulted in further improvement of both the tuning model and of neural control. These methods may enable robust neural control without needing to pause ongoing, practical use of BCIs, an important step toward clinical utility.

Acknowledgments

The authors would like to thank participants S3 and T1 and their families, The Boston Home and their staff, and John Simeral, Sergey Stavisky, Katie Centrella, Erin Gallivan, and Etsub Berhanu for their contributions to this study. Thanks also to Michael Black for comments on an earlier draft of the manuscript, to Naveen Rao, Steven Chase, and Wasim Malik for useful discussions, and to Laurie Barefoot, Beth Travers, and David Rosler for research support. Funding was provided by the Craig H Neilsen Foundation fellowship (BJ); Rehabilitation R&D Service, Department of Veterans Affairs (Merit Review Awards: B6453R and A6779I, Career Development Transition Award: B6310N, Senior Research Career Scientist Award: B6459L); NIH: NIDCD (R01DC009899), NINDS/NICHD (RC1HD063931), NICHD-NCMRR (N01HD53403, N01HD10018), NINDS-Javits (NS25074); the Doris Duke Charitable Foundation; the MGH-Deane Institute for Integrated Research on Atrial Fibrillation and Stroke; and the Katie Samson Foundation. The contents do not represent the views of the Department of Veterans Affairs or the United States Government.

Author contributions

BJ conceived the study design and CL decoder calibration method, and implemented them with NYM and DB. BJ and NYM designed and performed the data analyses and drafted the manuscript, which was further edited by all authors. SSC is clinical co-investigator of the pilot clinical trial and assisted in the clinical oversight of the participants. EE and GF

planned and executed the electrode array implants and supported the clinical research components of the study. JPD and LRH conceived, planned and continue to direct the ongoing BrainGate research. LRH is principal investigator of the BrainGate2 pilot clinical trial.

References

Bacher D, Jarosiewicz B, Masse N Y, Simeral J D, Donoghue J P and Hochberg L R 2011 Neural point-and-click communication by an individual with tetraplegia using the BrainGate intracortical neural interface system five years post-implant *Program No. 142.10. Neuroscience Meeting Planner* (Washington, DC: Society for Neuroscience)

Berger T W, Chapin J K, Gerhardt G A, McFarland D J, Principe J C, Soussou W V, Taylor D M and Tresco P A 2010 *Brain–Computer Interfaces: An International Assessment of Research and Development Trends* (Berlin: Springer)

Burrow M, Dugger J, Humphrey D R, Reed D J and Hochberg L R 1997 Cortical control of a robot using a time-delay neural network *Int. Conf. on Rehabilitation Robotics* pp 83–6

Carmena J M, Lebedev M A, Crist R E, O'Doherty J E, Santucci D M, Dimitrov D F, Patil P G, Henriquez C S and Nicolelis M A 2003 Learning to control a brain-machine interface for reaching and grasping by primates *PLoS Biol.* **1** E42

Chadwick E K, Blana D, Simeral J D, Lambrecht J, Kim S P, Cornwell A S, Taylor D M, Hochberg L R, Donoghue J P and Kirsch R F 2011 Continuous neuronal ensemble control of simulated arm reaching by a human with tetraplegia *J. Neural Eng.* **8** 034003

Chapin J K, Moxon K A, Markowitz R S and Nicolelis M A 1999 Real-time control of a robot arm using simultaneously recorded neurons in the motor cortex *Nature Neurosci.* **2** 583–4

Chapman C E and Meftah E M 2005 Independent controls of attentional influences in primary and secondary somatosensory cortex *J. Neurophysiol.* **94** 4094–107

Chase S M, Schwartz A B and Kass R E 2009 Bias, optimal linear estimation, and the differences between open-loop simulation and closed-loop performance of spiking-based brain-computer interface algorithms *Neural Netw.* **22** 1203–13

Chestek C A *et al* 2011 Long-term stability of neural prosthetic control signals from silicon cortical arrays in rhesus macaque motor cortex *J. Neural Eng.* **8** 045005

Churchland M M and Shenoy K V 2007 Temporal complexity and heterogeneity of single-neuron activity in premotor and motor cortex *J. Neurophysiol.* **97** 4235–57

Collinger J L, Wodlinger B, Downey J E, Wang W, Tyler-Kabara E C, Weber D J, McMorland A J C, Velliste M, Boninger M L and Schwartz A B 2013 High-performance neuroprosthetic control by an individual with tetraplegia *Lancet* **381** 557–64

Edeline J M 2003 The thalamo-cortical auditory receptive fields: regulation by the states of vigilance, learning and the neuromodulatory systems *Exp. Brain Res.* **153** 554–72

Ethier C, Oby E R, Bauman M J and Miller L E 2012 Restoration of grasp following paralysis through brain-controlled stimulation of muscles *Nature* **485** 368–71

Fetz E E 1969 Operant conditioning of cortical unit activity *Science* **163** 955–8

Fetz E E 2007 Volitional control of neural activity: implications for brain–computer interfaces *J. Physiol.* **579** 571–9

Fu Q-G, Flament D, Coltz J D and Ebner T J 1995 Temporal encoding of movement kinematics in the discharge of primate primary motor and premotor neurons *J. Neurophysiol.* **73** 836–54

Ganguly K and Carmena J M 2009 Emergence of a stable cortical map for neuroprosthetic control *PLoS Biol.* **7** e1000153

Ganguly K, Dimitrov D F, Wallis J D and Carmena J M 2011 Reversible large-scale modification of cortical networks during neuroprosthetic control *Nature Neurosc.* **14** 662–7

Georgopoulos A P, Kalaska J F, Caminiti R and Massey J T 1982 On the relations between the direction of two-dimensional arm movements and cell discharge in primate motor cortex *J. Neurosci.* **2** 1527–37

Gilja V *et al* 2012 A high-performance neural prosthesis enabled by control algorithm design *Nature Neurosci.* **15** 1752–7

Goldberg L R, Kercheval A N and Lee K 2005 t-statistics for weighted means in credit risk modelling *J. Risk Finance* **6** 349–65

Hauschild M, Mulliken G H, Fineman I, Loeb G E and Andersen R A 2012 Cognitive signals for brain–machine interfaces in posterior parietal cortex include continuous 3D trajectory commands *Proc. Natl Acad. Sci. USA* **109** 17075–80

Helms Tillery S I, Taylor D M and Schwartz A B 2003 Training in cortical control of neuroprosthetic devices improves signal extraction from small neuronal ensembles *Rev. Neurosci.* **14** 107–19

Hochberg L R, Serruya M D, Friehs G M, Mukand J A, Saleh M, Caplan A H, Branner A, Chen D, Penn R D and Donoghue J P 2006 Neuronal ensemble control of prosthetic devices by a human with tetraplegia *Nature* **442** 164–71

Hochberg L R *et al* 2012 Reach and grasp by people with tetraplegia using a neurally controlled robotic arm *Nature* **485** 372–5

Jarosiewicz B, Bacher D, Masse N Y, Hochberg L R and Donoghue J P 2012a Unsupervised filter calibration during ongoing use of the BrainGate2 neural interface by people with paralysis *Program No. 583.05. Neuroscience Meeting Planner* (New Orleans, LA: Society for Neuroscience)

Jarosiewicz B, Chase S M, Fraser G W, Velliste M, Kass R E and Schwartz A B 2008 Functional network reorganization during learning in a brain–computer interface paradigm *Proc. Natl Acad. Sci. USA* **105** 19486–91

Jarosiewicz B, Masse N Y, Bacher D, Hochberg L R and Donoghue J P 2011 Context dependence of neural tuning in motor cortex of people with paralysis: implications for neural prosthetics *Program No. 142.22. Neuroscience Meeting Planner* (Washington, DC: Society for Neuroscience)

Jarosiewicz B, Schummers J, Malik W Q, Brown E N and Sur M 2012b Functional biases in visual cortex neurons with identified projections to higher cortical targets *Curr. Biol.* **22** 269–77

Kakei S, Hoffman D S and Strick P L 1999 Muscle and movement representations in the primary motor cortex *Science* **285** 2136–9

Kim S, Wood F, Fellows M, Donoghue J P and Black M J 2006 Statistical analysis of the non-stationarity of neural population codes *1st IEEE/RAS-EMBS Int. Conf. on Biomedical Robotics and Biomechatronics* pp 811–6

Kim S P, Simeral J D, Hochberg L R, Donoghue J P and Black M J 2008 Neural control of computer cursor velocity by decoding motor cortical spiking activity in humans with tetraplegia *J. Neural Eng.* **5** 455–76

Kim S P, Simeral J D, Hochberg L R, Donoghue J P, Friehs G M and Black M J 2011 Point-and-click cursor control with an intracortical neural interface system by humans with tetraplegia *IEEE Trans. Neural Syst. Rehabil. Eng.* **19** 193–203

Koyama S, Chase S M, Whitford A S, Velliste M, Schwartz A B and Kass R E 2010 Comparison of brain-computer interface decoding algorithms in open-loop and closed-loop control *J. Comput. Neurosci.* **29** 73–87

Lebedev M A, Carmena J M, O'Doherty J E, Zacksenhouse M, Henriquez C S, Principe J C and Nicolelis M A L 2005 Cortical ensemble adaptation to represent velocity of an

artificial actuator controlled by a brain-machine interface *J. Neurosci.* **25** 4681–93
Li Z, O'Doherty J E, Lebedev M A and Nicolelis M A L 2011 Adaptive decoding for brain-machine interfaces through Bayesian parameter updates *Neural Comput.* **23** 3162–204
Malik W Q, Truccolo W, Brown E N and Hochberg L R 2011 Efficient decoding with steady-state Kalman filter in neural interface systems *IEEE Trans. Neural Syst. Rehabil. Eng.* **19** 25–34
Millán J R *et al* 2007 Adaptation in brain–computer interfaces *Toward Brain–Computer Interfacing* ed G Dornhege, J R Millán, T Hinterberger, D J McFarland and K-R Müller (Cambridge, MA: MIT Press) pp 279–90
Moritz C T, Perlmutter S I and Fetz E E 2008 Direct control of paralysed muscles by cortical neurons *Nature* **456** 639–42
Orsborn A, Dangi S, Moorman H and Carmena J 2012 Closed-loop decoder adaptation on intermediate time-scales facilitates rapid BMI performance improvements independent of decoder initialization conditions *IEEE Trans. Neural Syst. Rehabil. Eng.* **20** 468–77
Perge J A, Homer M L, Malik W Q, Cash S, Eskandar E, Friehs G, Donoghue J P and Hochberg L R 2013 Intra-day signal instabilities affect decoding performance in an intracortical neural interface system *J. Neural Eng.* **10** 036004
Reynolds J H and Chelazzi L 2004 Attentional modulation of visual processing *Annu. Rev. Neurosci.* **27** 611–47
Roesch M R and Olson C R 2004 Neuronal activity related to reward value and motivation in primate frontal cortex *Science* **304** 307–10
Santhanam G, Linderman M D, Gilja V, Afshar A, Ryu S I, Meng T H and Shenoy K V 2007 HermesB: a continuous neural recording system for freely behaving primates *IEEE Trans. BioMed. Eng.* **54** 2037–50
Santhanam G, Ryu S I, Yu B M, Afshar A and Shenoy K V 2006 A high-performance brain-computer interface *Nature* **442** 195–8
Schlögl A, Vidaurre C and Müller K-R 2010 Adaptive methods in BCI research—an introductory tutorial *Brain–Computer Interfaces: The Frontiers Collection* ed B Graimann, G Pfurtscheller and B Allison (Berlin: Springer) pp 331–55
Schwartz A B, Kettner R E and Georgopoulos A P 1988 Primate motor cortex and free arm movements to visual targets in three-dimensional space: I. Relations between single cell discharge and direction of movement *J. Neurosci.* **8** 2913–27
Sergio L E and Kalaska J F 1998 Changes in the temporal pattern of primary motor cortex activity in a directional isometric force versus limb movement task *J. Neurophysiol.* **80** 1577–83
Serruya M D, Hatsopoulos N G, Paninski L, Fellows M R and Donoghue J P 2002 Instant neural control of a movement signal *Nature* **416** 141–2
Shpigelman L, Lalazar H and Vaadia E 2009 Kernel-ARMA for hand tracking and brain–machine interfacing during 3D motor control *Advances in Neural Information Processing Systems* ed D Koller, D Schuurmans, Y Bengio and L Bottou (Cambridge, MA: MIT Press) p 21
Simeral J D, Kim S P, Black M J, Donoghue J P and Hochberg L R 2011 Neural control of cursor trajectory and click by a human with tetraplegia 1000 days after implant of an intracortical microelectrode array *J. Neural Eng.* **8** 25027
Sussillo D, Nuyujukian P, Fan J M, Kao J C, Stavisky S D, Ryu S and Shenoy K 2012 A recurrent neural network for closed-loop intracortical brain–machine interface decoders *J. Neural Eng.* **9** 026027
Taylor D M, Helms Tillery S I and Schwartz A B 2002 Direct cortical control of 3D neuroprosthetic devices *Science* **296** 1829–32
Taylor J R 1996 *An Introduction to Error Analysis: The Study of Uncertainties in Physical Measurements* (Sausalito, CA: University Science Books)
Velliste M, Perel S, Spalding M C, Whitford A S and Schwartz A B 2008 Cortical control of a prosthetic arm for self-feeding *Nature* **453** 1098–101
Wahnoun R, He J and Helms Tillery S I 2006 Selection and parameterization of cortical neurons for neuroprosthetic control *J. Neural Eng.* **3** 162–71
Wessberg J and Nicolelis M A L 2006 Optimizing a linear algorithm for real-time robotic control using chronic cortical ensemble recordings in monkeys *J. Cogn. Neurosci.* **16** 1022–35
Wu W, Gao Y, Bienenstock E, Donoghue J P and Black M J 2006 Bayesian population decoding of motor cortical activity using a Kalman filter *Neural Comput.* **18** 80–118
Zhang Y, Meyers E M, Bichot N P, Serre T, Poggio T A and Desimone R 2011 Object decoding with attention in inferior temporal cortex *Proc. Natl Acad. Sci. USA* **108** 8850–5